

Exchange Reaction Kinetics and Geospeedometry*

Ye. A. Mitina, L. M. Truskinovskiy and E. E. Senderov

Vernadskiy Institute of Geochemistry and Analytical Chemistry, USSR Academy of Sciences

A new approach based on exchange-reaction thermodynamics is proposed for research on rock composition changes during thermal evolution. Kinetic equations of Onsager type apply, which related the reaction rate to the deviation from equilibrium. In the case of two-component cation exchange between two solid phases, a relation exists between the kinetic coefficient and the self-diffusion coefficients for the components in the two phases, the equilibrium constant, the phase sizes, and its temperature dependence. The model has been applied to rates of cooling of metamorphic rocks and to correcting and interpreting readings from ion-exchange geothermometers. The results of modelling the compositions of the garnet-clinopyroxene pair, which shows Mg-Fe²⁺ exchange during continuous cooling, enables us to estimate the rates and times of thermal events. It is possible to use exchangeable-component concentrations averaged over grains as geospeedometers. This approach is applied to studying reactions to obtain independent kinetic characteristics that can be used to examine various types of mineral reaction during metamorphism.

Geothermometry, based on measurements on ion-exchange and isotope equilibria, is widely used to recover the thermal history of rocks. Use of the method is based on equilibrium thermodynamics, which relates the compositions of coexisting phases to pressure and temperature. If equilibrium is attained and persists, the compositions reflect the P and T, but effects from preceding processes are lost.

There are frequently major constraints associated with transformation kinetics. The main problems here are related to how the quenched concentrations are dependent on the cooling rate, and the extent to which the system remembers the initial temperature and the concentration zonation. In that respect, geothermometry is closely related to geospeedometry, so one can consider conditions of origins and subsequent thermal history together. In rate studies, the task of recovering the temperature is transformed into one of recovering the T-t path of the system [1, 2].

Here we need to solve simultaneously the kinetic equation for the relaxation of internal parameters to the equilibrium values and the equation describing the evolution of the temperature field [1, 2]. When one simulates zonation in minerals associated with element exchange one considers mainly two types of reaction: diffusion of the main cations in rock-forming minerals such as Fe²⁺ and Mg and the distributions of trace components between coexisting phases, e.g., Zr in ilmenite and ulvospinel [3-13].

Several studies have been done [5, 7, 14, 15] on the mechanism of cation exchange and the role of factors that influence the readings of ion-exchange geothermometers. Equations have been derived for mineral pairs that govern the kinetic response in an ion-exchange geothermometer to any changes in T-t behavior related to the mineral sizes and shapes. The diffusion profile and diffusion-zone width are determined for a given pair by the diffusion coefficients, exchange

*Translated from *Geokhimiya*, No. 10, pp. 1372-1386, 1991.

enthalpy, initial conditions, and cooling history. In particular, the absence of zonation is not a guarantee of equilibrium for geothermometers based on garnet-pyroxene and olivine-spinel pairs, e.g., slowly cooling rocks show almost no concentration gradients. When the diffusion rate for the cations in one mineral differs considerably from that in the adjacent one, the applicability of a geothermometer is controlled by the mineral with the lower diffusion coefficient in the working temperature range.

Here we consider a new approach to the change in rock composition during thermal evolution. A kinetic equation is proposed that relates the reaction rate to the deviation from equilibrium. That equation relates the characteristic transformation time to the grain size and the diffusion coefficients in the coexisting phases. It enables one to examine the kinetics no matter what the initial state and allows one to estimate the effects from the uncertainty of data on the diffusion rates on estimates of the cooling rate. The model operates with component concentrations averaged over grains. These are used as thermal-history indicators to reduce the difficulties associated with measuring composition profiles, particularly of small grains. An example is considered of reaction between garnet and clinopyroxene. The kinetic equations are used to recover the cooling rates from the frozen composition of the minerals.

KINETIC EQUATIONS

Let us consider an assemblage composed of r phases, each of which is an n -component solid solution ($r \leq n + 2$). By C_a^i we denote the molar fraction of component i ($i = 1, \dots, n$) in phase a ($a = 1, \dots, r$), while ξ^a is the molar fraction of phase a in the mixture. For exchange reactions, the independent reaction degrees of freedom can be taken as the concentrations C_a^i , $i = 1, \dots, n - 1$ of the components in the $r - 1$ phases (where there are various possible sets of $r - 1$ phases).

$$dG = \sum_{\alpha=1}^{(r-1)(n-1)} \frac{\partial G}{\partial \zeta_{\alpha}} d\zeta_{\alpha}, \quad (1)$$

The increment in the Gibbs free energy for the assemblage is

in which ζ_{α} , $\alpha = 1, \dots, (r - 1)(n - 1)$ are the generalized internal parameters, e.g.,

$$\zeta_{\alpha} = \{\xi^a C_a^i\}_{r-1}^{n-1}. \quad (2)$$

The internal parameters can be taken as the products ξ_c of the phase proportions and the component concentrations, namely independent combinations of the variables ζ_{α} . For example, for an exchange reaction in a binary solution, the number of internal parameters ζ_{α} is $(r - 1)(n - 1) = 1$, so one can use the concentration of one component in the two phases alone.

Using an algorithm from the linear thermodynamics of irreversible processes [15], we can write a simple kinetic equation for the relaxation of the parameters $\zeta_{\alpha} = \{\xi^a C_a^i\}$ to the equilibrium values:

$$\frac{d\zeta_{\alpha}}{dt} = - \sum_{\beta} K_{\alpha\beta} \frac{\partial G}{\partial \zeta_{\beta}}, \quad (3)$$

in which $K_{\alpha\beta}$ is a symmetrical positive-definite matrix containing the kinetic coefficients, whose components are functions of pressure, temperature, and the overall mixture composition. The temperature dependence is usually of Arrhenius type:

$$K(T) = K_0 \exp\left(-\frac{\Delta H}{RT}\right), \quad (4)$$

in which ΔH is the activation enthalpy and K_0 the frequency factor. The cross coefficients $K_{\alpha\beta}$ ($\alpha \neq \beta$) define the dependence of the rate of reaction α on the extent of equilibration in reaction β . We can explain the coefficients in K if we neglect the cross kinetic effects and take the matrix as diagonal. Matrices K and G can be reduced simultaneously to diagonal forms, and G is also taken as diagonal. Then the (3) system near the equilibrium state is written as

$$\frac{d\zeta_\alpha}{dt} = -K_{\alpha\alpha} \frac{\partial^2 G}{\partial \zeta_\alpha^2} \Big|_{P^*, T^*} \cdot (\zeta_\alpha - \zeta_\alpha^*), \quad (5)$$

$$\alpha = 1, \dots, (r-1)(n-1).$$

Here $\tau_\alpha = (K_{\alpha\alpha} \partial^2 G / \partial \zeta_\alpha^2)^{-1}$ specifies the characteristic kinetic time-scale for reaction α .

In the case of an ideal binary solution, we take $\zeta_\alpha \equiv \xi^a C_a^i$, and the rate of change in C_a^i is [12]

$$\frac{dC_a^i}{dt} = -\frac{K}{\xi^a} \left(RT \ln \frac{C_a^i (1 - C_b^i)}{(1 - C_a^i) C_b^i} - \Delta g(P, T) \right). \quad (6)$$

Here $K > 0$ is the kinetic-coefficient matrix, while ξ^a is given by

$$C_a^i \xi^a + C_b^i (1 - \xi^a) = C^0$$

in which C^0 is the overall mixture composition and $\Delta g(P, T)$ is the standard molar free energy.

As the ξ^a are fixed, C_b^i is a function of C_a^i :

$$C_b^i = \frac{C^0 - C_a^i \xi^a}{1 - \xi^a}. \quad (7)$$

Substituting this into Eq. (6), we transform it to

$$\frac{dC_a^i}{dt} = -\frac{K}{\xi^a} RT \left(\ln \frac{C_a^i (1 - \xi^a - C^0 + C_a^i \xi^a)}{(1 - C_a^i) (C^0 - C_a^i \xi^a)} - \frac{\Delta g(P, T)}{RT} \right). \quad (8)$$

When the reaction occurs near equilibrium, we can obtain a linearized form for Eq. (8). Let C_a^{eq} be the equilibrium composition for the given T, P, C , and ξ^a , which satisfies

$$\frac{dC_a^i}{dt} \Big|_{C_a^i = C_a^{eq}} = 0, \quad (9)$$

$$\Delta g^a(P, T) = RT \ln \frac{C_a^{eq} (1 - \xi^a - C^0 + C_a^{eq} \xi^a)}{(1 - C_a^{eq}) (C^0 - C_a^{eq} \xi^a)}.$$

(For a binary solution as considered here, we omit the i and a and take C^{eq} and C as the concentrations of component i in phase a .)

Then

$$\begin{aligned} \frac{dC}{dt} &= -\frac{K}{\xi} RT \ln \left(\frac{C (1 - \xi - C^0 - C\xi) (1 - C^{eq}) (C^0 - C^{eq}\xi)}{(1 - C) (C^0 - C\xi) C^{eq} (1 - \xi - C^0 - C^{eq}\xi)} \right) = \\ &= -\frac{K}{\xi} RT f(\xi, C, C^0, C^{eq}) \end{aligned} \quad (10)$$

(the logarithm on the RHS is denoted by $f(\xi, C, C^0, C^{eq})$. When the deviation from equilibrium is small ($C = C^{eq} + \xi$, where $\xi \ll 1$), Eq. (10) is converted to linear form:

$$\frac{dC}{dt} = -\frac{K}{\xi} RT (C - C^{eq}) F(\xi, C^0, C^{eq}). \quad (11)$$

Here

$$F(\xi, C^0, C^{eq}) = \frac{C^0(1-\xi) + C^0{}^2 + 2CC^{eq}\xi - C^{eq}{}^2\xi}{C^{eq}(1-C^{eq})(C^0 - C^{eq}\xi)(1-\xi - C^0 + C^{eq}\xi)}. \quad (12)$$

To close the model and calculate the $K_{\alpha\beta}$, phenomenological consideration is inadequate, and one needs a microscopic model for the component redistribution between phases.

EXCHANGE-REACTION MECHANISM

We derived the dependence of K in Eqs. (10) and (11) on the diffusion coefficients, grain sizes, and equilibrium constant from a simple model of redistribution of components between two phases.

The zonation observed in grains of coexisting minerals is due to cations diffusing from one mineral to the other in response to temperature change. The transport direction is governed by the temperature dependence of the distribution coefficient. Retention of concentration gradients near boundaries between grains indicates that the exchange is incomplete, i.e., the reaction rate has fallen so much, e.g., in response to falling temperatures, that the compositions have been quenched. The concentration profiles should thus be determined by the cooling history and can be used to reconstruct the T-t path. We need to solve diffusion equations for the cation transport having first determined the geometry (i.e., grain shape and size) together with the boundary and initial conditions.

Let us examine a one-dimensional model as a layered medium with phases a and b alternating (Fig. 1). It is symmetrical, so we will consider two contacting grains of phases a and b . Let l be the characteristic size of the two-phase layer, while ξl is the size of the grain of phase a and $(1 - \xi)l$ is that of phase b . Neglecting the difference in the molar volumes, we assume that ξ^a coincides with the volume fraction [7].

The physical assumptions are: I. At a certain initial temperature T_0 , the two phases are in a state of chemical equilibrium; II. During cooling, local equilibrium is set up at each instant at the boundary. III. Only the two cations 1 and 2 (e.g., Fe^{2+} and Mg^{2+}) are exchanged, and the concentrations of all the other elements are unaltered.

Let $C_\varphi^i(x, t)$ be the concentrations of component i in phase φ at a distance x from the boundary at time t . The I equilibrium conditions at the start are:

$$C_\varphi^i(x, 0) = C_\varphi^i = \text{const}, \quad (13)$$

$$\frac{C_a^1 C_b^2}{C_b^1 C_a^2} = \kappa_0(T_0),$$

where κ_0 is the equilibrium constant at T_0 . The conditions at the II boundary are:

$$\frac{C_a^1(0, t) \cdot C_b^2(0, t)}{C_b^1(0, t) \cdot C_a^2(0, t)} = \kappa(T). \quad (14)$$

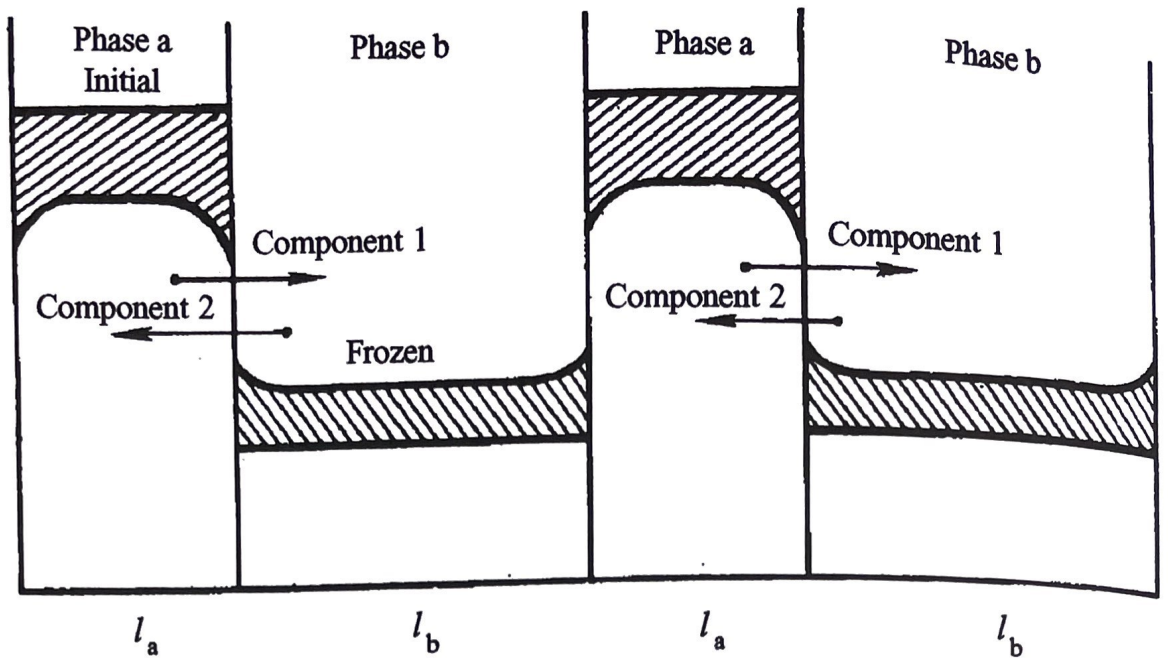


Fig. 1. Schematic representation of frozen concentration profiles for an exchanging component after the completion of the exchange in a layered system containing alternating phases a and b .

Neglecting the effect due to deviations from ideal behavior in the phases, we assume that $\kappa(T)$ is $\kappa(T) = \kappa_{\infty} e^{-\Delta H^0/RT}$, in which κ_{∞} is $\kappa(T)$ for $T \rightarrow \infty$ and ΔH^0 is the standard molar enthalpy of the exchange, which in general is dependent on T , P , and the coexisting-phase compositions. However, if the composition and temperature ranges are narrow, one can take ΔH^0 as constant.

Conservation of matter during the exchange requires equal component fluxes at the boundary. The flux $J_{\phi}^i(x)$ of component i in phase ϕ at a distance x from the boundary is given by Fick's first law:

$$J_{\phi}^i(x) = -D_{\phi}^i(T) \frac{\partial C_{\phi}^i}{\partial x}, \quad (15)$$

in which $D_{\phi}^i(T)$ is the diffusion coefficient for ion i in phase ϕ at temperature t , so

$$\begin{aligned} D_a^1(T) \frac{\partial C_a^1}{\partial x} \Big|_{x=0} &= -D_a^2(T) \frac{\partial C_a^2}{\partial x} \Big|_{x=0} = \\ &= D_b^1(T) \frac{\partial C_b^1}{\partial x} \Big|_{x=0} = -D_b^2(T) \frac{\partial C_b^2}{\partial x} \Big|_{x=0}. \end{aligned} \quad (16)$$

Here x is the positive distance from the boundary and the D are normalized on the basis of the differences in molar volumes and cation contents in the phases. We subsequently assume that the exchange is limited by diffusion in the bulk of the grains. Our one-dimensional model involves the assumptions that the radius of curvature of the phase boundary is large by comparison with the diffusion distance and that the direction of the concentration gradient coincides with the normal to the common boundary. Therefore, we need to consider only the component of the diffusion tensor in the x direction.

The rate of change in the concentration of cation i at point (x, t) is

$$\frac{\partial C_{\phi}^i(x, t)}{\partial t} = \frac{\partial}{\partial x} \left(D_{\phi}^i(T) \frac{\partial C_{\phi}^i(x, t)}{\partial x} \right). \quad (17)$$

As there is mutual diffusion between the components, the diffusion coefficients are the mutual diffusion ones D_φ for a pair of ions in each phase. The temperature dependence of those coefficients is $D_\varphi = D_\varphi^\infty \exp(-\Delta E_\varphi^0/RT)$, in which ΔE_φ^0 is the diffusion activation energy, which is taken as constant along with D_φ^∞ within the relevant composition and temperature ranges. Also, the composition dependence of D_φ and thus the x dependence will be neglected. The molar concentrations are related by the electrical neutrality conditions $C_\varphi^1(x, t) + C_\varphi^2(x, t) = \text{const}$ for all φ, x , and t , so the concentration profiles for components 1 and 2 are simply mirror images with respect to the phase boundary. This means that we need consider only one component in each phase, e.g., Fe^{2+} (component 1).

As the grain sizes are small, we cannot always measure the composition profiles, and in those cases we can use their means over the volumes, i.e.,

$$\bar{C}_a^1 = \frac{1}{\xi l} \int_{-\xi l}^0 C_a^1(x) dx, \quad \bar{C}_b^1 = \frac{1}{(1-\xi)l} \int_0^{(1-\xi)l} C_b^1(x) dx. \quad (18)$$

On account of the symmetry of the profiles about the centers of the grains,

$$\bar{C}_a^1 = \frac{2}{\xi l} \int_{-\xi l/2}^0 C_a^1(x) dx, \quad \bar{C}_b^1 = \frac{2}{(1-\xi)l} \int_0^{(1-\xi)l/2} C_b^1(x) dx. \quad (19)$$

The conditions for symmetry of the profiles at the points $-\xi l/2$ and $(1-\xi)l/2$ physically denote the absence of component fluxes at those points:

$$\left. \frac{\partial C_a^1}{\partial x} \right|_{x=-\xi l/2} = 0, \quad \left. \frac{\partial C_b^1}{\partial x} \right|_{x=(1-\xi)l/2} = 0. \quad (20)$$

For a given phase composition, $\xi = \text{constant}$, differentiation of Eq. (19) gives

$$\begin{aligned} \frac{\partial}{\partial t} \bar{C}_a^1(t) &= \frac{2}{\xi l} \int_{-\xi l/2}^0 \frac{\partial C_a^1}{\partial t} dx = \frac{2}{\xi l} D_a(T) \int_{-\xi l/2}^0 \frac{\partial^2 C_a^1}{\partial x^2} dx = \\ &= \frac{2}{\xi l} D_a(T) \left. \frac{\partial C_a^1}{\partial x} \right|_{x=0}, \end{aligned} \quad (21)$$

$$\frac{\partial}{\partial t} \bar{C}_b^1(t) = \frac{2}{(1-\xi)l} D_b(T) \left. \frac{\partial C_b^1}{\partial x} \right|_{x=0} = -\frac{2}{(1-\xi)l} D_b(T) \left. \frac{\partial C_b^1}{\partial x} \right|_{x=0}. \quad (22)$$

The condition for equal fluxes at the boundary gives a relation for the mean concentrations:

$$\left(\frac{\partial}{\partial t} \bar{C}_a^1 \right) \frac{\xi l}{2} = - \left(\frac{\partial}{\partial t} \bar{C}_b^1 \right) \frac{(1-\xi)l}{2} \quad (23)$$

or after integration

$$\bar{C}_a^1(t) \xi + \bar{C}_b^1(t) (1-\xi) = \text{const} = C^1, \quad (24)$$

in which C^0 are defined from the initial conditions:

$$\overset{0}{C}_a^1 \xi + \overset{0}{C}_b^1 (1 - \xi) = \overset{0}{C}^1. \quad (25)$$

The mean compositions are thus related by component balance conditions. The internal parameter can be taken as $\bar{C}_a^1(t)$. One analyzes the model equations to get an ordinary differential equation for $\bar{C}_a^1(t)$ to relate the coefficients in that equation to the D_φ , phase sizes, overall composition, and equilibrium constant.

The following are the equations for the model together with the initial and boundary conditions.

1. Diffusion equations:

$$\begin{aligned} \frac{\partial C_a^1}{\partial t} &= D_a(T) \frac{\partial^2 C_a^1}{\partial x^2}, & x \in [-\xi l/2, 0]; \\ \frac{\partial C_b^1}{\partial t} &= D_b(T) \frac{\partial^2 C_b^1}{\partial x^2}, & x \in [0, (1-\xi)l/2]. \end{aligned} \quad (26)$$

2. Initial conditions:

$$\begin{aligned} \overset{0}{C}_a^1 &= \text{const}, \quad \overset{0}{C}_b^1 = \text{const}; \\ \frac{\overset{0}{C}_a^1 \overset{0}{C}_b^2}{\overset{0}{C}_b^1 \overset{0}{C}_a^2} &= \kappa(T_0) = \kappa_0; \end{aligned} \quad (27)$$

$$\overset{0}{C}_a^1 \xi + \overset{0}{C}_b^1 (1 - \xi) = \overset{0}{C}^1,$$

in which the parameters C_a^1 and C_b^1 are related to C_a^2 and C_b^2 by

$$C_\varphi^1 + C_\varphi^2 = \text{const} = \overset{0}{C}_\varphi^1 + \overset{0}{C}_\varphi^2 = \overset{0}{C}_\varphi, \quad \varphi = a, b. \quad (28)$$

3. Boundary conditions:

$$\begin{aligned} \frac{\partial C_a^1}{\partial x} &= 0, & x = -\xi l/2; \\ \frac{\partial C_b^1}{\partial x} &= 0, & x = (1-\xi)l/2; \\ D_a(T) \frac{\partial C_a^1}{\partial x} &= -D_b(T) \frac{\partial C_b^1}{\partial x}, & x = 0; \\ \frac{C_a^1(0, t) C_b^2(0, t)}{C_b^1(0, t) C_a^2(0, t)} &= \kappa(T). \end{aligned} \quad (29)$$

In what follows, we are interested not in the solution $C_a^1(x, t)$ to that system (which in particular demonstrates zonation) but in the behavior of the integral characteristic

$$\bar{C}_a^1(t) = \frac{2}{\xi l} \int_{-\xi l/2}^0 C_a^1(x) dx. \quad (30)$$

ISOTHERMAL KINETICS

An isothermal process occurs as follows. At a certain temperature T_0 , the system is in equi-

librium, and the component concentrations in the two phases are constant at their equilibrium values for T_0 . At time $t = 0$, the temperature changes by ΔT , and the equilibrium is perturbed: the concentrations at the phase boundary alter and the flux of a component occurs through the boundary, with the system relaxing to the new equilibrium distribution under isothermal conditions at $T = T_0 - \Delta T$.

Let us rewrite Eq. (27) with the dimensionless variable $x' = x/l$ and $t' = tD_b/l^2$:

$$\begin{aligned} \frac{\partial C_a^1}{\partial t'} &= \frac{D_a}{D_b} \frac{\partial^2 C_a^1}{\partial x'^2}, & x' \in [-\xi/2, 0]; \\ \frac{\partial C_b^1}{\partial t'} &= \frac{\partial^2 C_b^1}{\partial x'^2}, & x' \in [0, (1-\xi)/2]. \end{aligned} \quad (31)$$

$$C_a^1(x', 0) = \overset{0}{C}_a^1, \quad C_b^1(x', 0) = \overset{0}{C}_b^1; \quad \frac{\overset{0}{C}_a^1 \overset{0}{C}_b^2}{\overset{0}{C}_b^1 \overset{0}{C}_a^2} = \kappa_0, \quad (32)$$

in which

$$\overset{0}{C}_a^2 = \overset{0}{C}_a - \overset{0}{C}_a^1, \quad \overset{0}{C}_b^2 = \overset{0}{C}_b - \overset{0}{C}_b^1, \quad C_a^1 \xi + C_b^1 (1 - \xi) = \overset{0}{C}^1; \quad (33)$$

$$\begin{aligned} \frac{\partial C_a^1}{\partial x'}(-\xi/2, t') &= 0; \\ \frac{\partial C_b^1}{\partial x'}((1-\xi)/2, t') &= 0; \end{aligned} \quad (34)$$

$$\begin{aligned} \frac{D_a}{D_b} \frac{\partial C_a^1}{\partial x'}(0^-, t') &= \frac{\partial C_b^1}{\partial x'}(0^+, t'); \\ \frac{C_a^1(0, t') C_b^2(0, t')}{C_b^1(0, t') C_a^2(0, t')} &= \kappa(T) = \kappa. \end{aligned}$$

The concentrations are expressed in mol.%, so the dimensionless parameters are D_a/D_b , ξ , κ , κ_0 , $\overset{0}{C}_a^1$, $\overset{0}{C}_b^1$. The last three define only the initial state, so the parameters in Eq. (10) should be dependent only on ξ , D_a/D_b , and κ .

Numerical solution of Eq. (34) enabled us to check Eq. (10) and the linear analog Eq. (11) for the relaxation to equilibrium at constant temperature.

Figure 2 shows the numerical results. Lines 1 and 2 describe $d\bar{C}_a^1(t)dt$ during relaxation, where $C_a^1 - C_a^{eq}$ defines the thermodynamic force (here C_a^{eq} are the equilibrium concentrations of component 1 in phase a). Line 1 is from Eq. (10) and line 2 from Eq. (11). Near equilibrium, namely ~90% conversion, the rate of change in the mean concentration is proportional to the degree of conversion. Curves 1 and 2 have a common linear section at small $C_a^1 - C_a^{eq}$. This result indicates that the kinetic behavior of the pair at small deviations from equilibrium follows Eq. (11). The kinetic coefficient K is defined by the slope of the linear part of curve 1 in Fig. 2a:

$$\tan \alpha = \frac{l^2}{D_b} (KRT/\xi) F(\xi, \overset{0}{C}_a^1, C_a^{eq}).$$

Figure 2b shows the lines for various initial temperatures $T_2^0 < T_1^0$, which coincide as equilibrium is approached. The relaxation rate on approach to equilibrium is independent of the initial state.

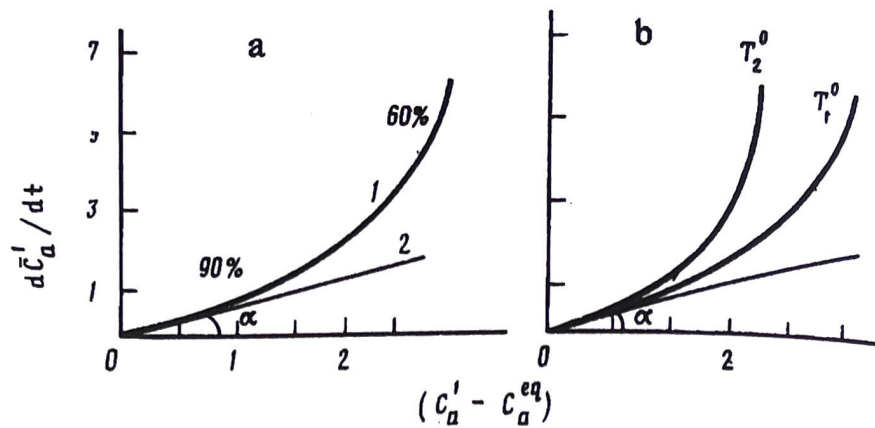


Fig. 2. Rates of change of mean concentration in relation to deviation from equilibrium: a) 1) from (10); 2) from (11); b) $T_2^0 < T_1^0$ lines corresponding to various initial temperatures in Eq. (10).

We can thus examine how the dimensionless kinetic parameter in Eq. (11) behaves:

$$\tilde{K} = (l^2/D_b)KRT \quad (35)$$

as a function of the characteristic parameters in the Eq. (34) model: D_a/D_b , ξ , and κ , whose values may be varied.

We determined the kinetic coefficients for the ranges $10^{-2} \leq D_a/D_b \leq 10^2$, $0.1 \leq \xi \leq 0.9$, and $0.1 \leq \kappa \leq 1$. Figure 3 shows lines 1-3 corresponding to ξ of 0.1, 0.5, and 0.9. The solid lines correspond to $\kappa = 0.1$ and the dashed ones to $\kappa = 1$.

If the relation between the diffusion coefficients is $D_a < D_b$, \tilde{K} (the reaction rate near equilibrium) is higher for the system with the lower ξ , and conversely for $D_a > D_b$, it is higher the larger the x for the phase with the larger diffusion coefficient D_a . Near $D_a \approx D_b$, \tilde{K} is independent of the phase sizes. It is also proportional to the reciprocal of the reaction time: $\tilde{K} \propto 1/\tau = l^2/D_b t$ (we use $L \propto \sqrt{Dt}$ for the width of the diffusion zone).

In the first case, $D_a/D_b \ll 1$, the limiting phase is phase a , with grain size $L = \xi l$ so $\tilde{K} \propto (D_a/D_b)/\xi^2$, i.e., \tilde{K} increases as ξ decreases.

When $D_a/D_b \gg 1$, the limiting phase is b , with grain size $L = (1 - \xi)l$, and then $\tilde{K} \propto 1/(1 - \xi)^2$, which means that \tilde{K} increases with ξ . Also, starting at a certain D_a/D_b , \tilde{K} ceases to be dependent on D_a/D_b . In Fig. 3, this corresponds to the flat parts of the $\xi = \text{constant}$ curves for $D_a/D_b > 10^2$.

When $D_a/D_b \approx 1$, the process is limited by bulk diffusion in the two phases, $L = l$, $\tilde{K} \text{ const.}$, i.e., is independent of the relation between the grain sizes.

Figure 3 shows that \tilde{K} is only slightly dependent on κ because the dependence has already been incorporated in the expression for the thermodynamic driving force.

The linear variation in exchange rate near equilibrium at constant temperature indicates that this model is suitable for describing exchange between phases. The T dependence of \tilde{K} is due to the T dependence of D , which we use with the assumption that it takes the form $\tilde{K}(T) = \tilde{K}_0 RT \exp(-\Delta H_c/RT)$, which enables us to relate the enthalpy of reaction ΔH_c to the diffusion activation energies in the two phases. This means that Eq. (11) can be used for the nonisothermal case, i.e., we can

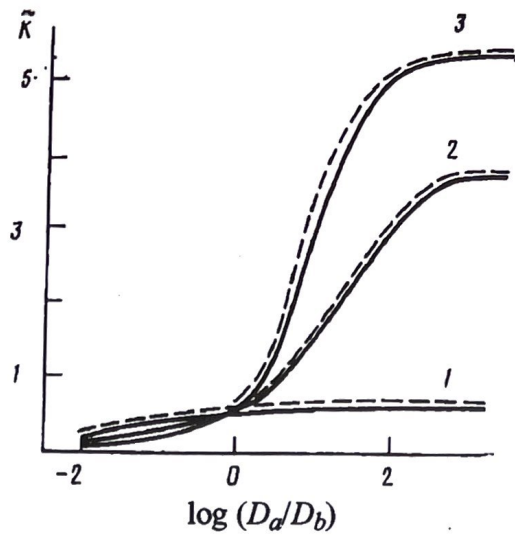


Fig. 3. Dependence of \tilde{K} in Eq. (11) on D_a/D_b , ξ , and κ . Lines 1-3 correspond to the proportions of phase a for ξ of 0.1, 0.5, and 0.9. Solid lines $\kappa = 0.1$, dashed lines $\kappa = 1$.

determine the temperature conditions and evaluate the role of each kinetic parameter on the basis of the mean composition, not the zonation.

NONISOTHERMAL KINETICS

T may vary for example because rocks rise or sink or from cooling after eruption and so on.

The behavior of $\bar{C}_a^1(t)$ will be examined by solving Eq. (34) with a given law for the change in temperature $T(t)$, which enters into Eq. (34) via $\kappa(T(t))$ and $D_a(T(t))$ and $D_b(T(t))$. The resulting $\bar{C}_a^1(t)$ must be compared with the solution found by using the kinetic coefficients in (10) and (11).

We examined Fe^{2+} -Mg exchange in the garnet-clinopyroxene pair:



A study has been made [7] on how the exchange here is affected by the ratio of the D , by ΔH , the crystal size, and the cooling rates as regards the concentration distributions and the shapes of the zoned profiles. We have used those results to test our method and model. Figure 4a shows the frozen Fe^{2+} profiles for clinopyroxene derived by solving Eq. (34). The main parameters were taken from [7]. The cooling law was $T(t) = T_0 - St$, with $T_0 = 1473$ K and $S = 10$ K/My. As $C_a^1(t)$ we took the Fe^{2+} concentration in the clinopyroxene.

Figure 4b shows $\bar{C}_a^1(t)$ for that cooling and also the quenching time and the frozen values of the mean concentration corresponding to the Fig. 4a diffusion profile.

The dimensionless isothermal treatment has shown that the relaxation rate near equilibrium is dependent only on ξ , D_a/D_b , and κ and is independent of the initial conditions (Fig. 2). We performed calculations for isothermal conditions $T = \text{const}$ (1400, 1300, 1200, 1100, and 1000 K) with various T_0 , and Fig. 5a shows the rate of change in the mean concentration as a function of the deviation from equilibrium with $x = d\bar{C}_a^1/dt$ and $y = \bar{C}_a^1 - C_a^{eq}$ as axes; the solid lines are for 1000 K and the dashed ones for 1100 K. Figure 5b illustrates the independence of the conversion

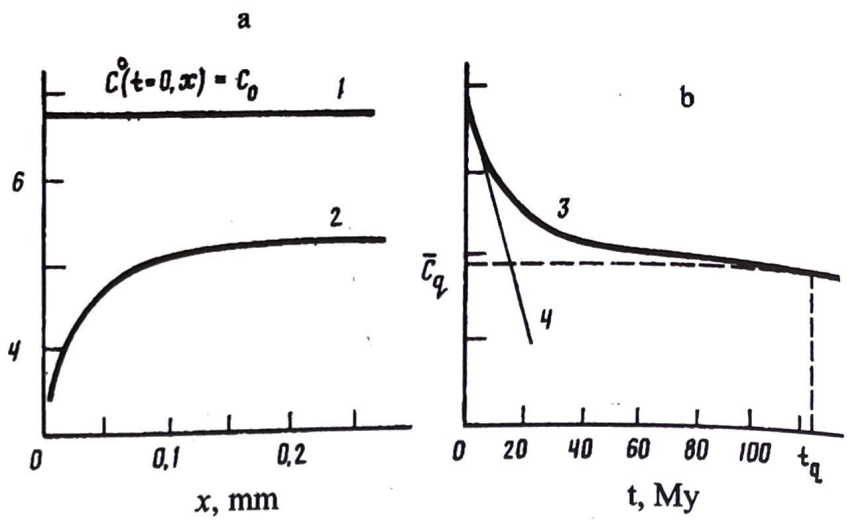


Fig. 4. Concentration profiles for exchanging component and variations in mean concentration during cation exchange ($T = T_0 - St$, $T_0 = 1473$ K/My): a) 1) initial Fe^{2+} distribution in clinopyroxene; 2) frozen profiles; b) 3) change in mean concentration; 4) equilibrium curve.

rate from the initial temperature ($T_0 = 1500 - 1350$ K) near equilibrium at 1300 K.

The slope of the linear part of Fig. 5c for small $\bar{C}_a^1(t) - C_a^{eq}$ defines \tilde{K} .

For $T = \text{constant}$, Eq. (11) can be integrated:

$$\bar{C}(t) = C^{eq}(T) + (\bar{C}(0) - C^{eq}(T)) \exp(-kt), \quad (37)$$

in which

$$k = KRT \frac{1}{\xi} F(\xi, \bar{C}, C^{eq}) = \text{const for } \xi, T = \text{const}$$

(k has the dimensions of reciprocal time, $\tilde{K} = k^2/D_b$).

The \tilde{K} derived from the calculations (Fig. 5) serve to define how well Eq. (37) describes the solution to Eq. (34). Figure 6 shows lines corresponding to the Eq. (37) solution (line 1) and the Eq. (34) one, line 2 ($T = 1300$ K, $T_0 = 1400$, and 1500 K), which almost coincide after a certain time.

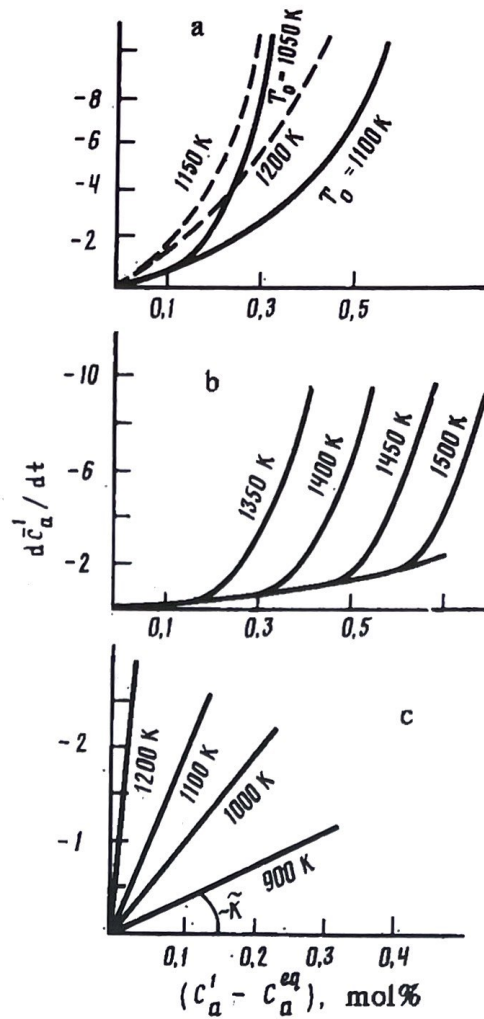
The temperature dependence of $K = \xi k/RTF$ can be derived by constructing a fitting line: $\ln K = \ln K_0 - \Delta H_c/RT$, where $K_0 \approx 5 \cdot 188 \text{ sec}^{-1}$ and $\Delta H_c 83 448 \text{ cal/mol}$ (Fig. 7).

The isothermal kinetic equation is (10), which is of first order, and the parameters of its temperature dependence have been derived for it. This enables us to examine the behavior of the transformation of varying temperatures.

The solution to Eq. (11) for $T = T(t)$ is represented in quadratures:

$$\bar{C}(t) = \left[\bar{C}(0) + \int_0^t \exp(-A(\tau)) C^{eq}(\tau) k(\tau) d\tau \right] \exp A(t), \quad (38)$$

Fig. 5. Rates of Fe^{2+} -Mg exchange between garnet and clinopyroxene under isothermal conditions: a) solid lines $T = 1000$ K, dashed lines $T = 1100$ K for two initial temperatures; b) $T = 1300$ K for four initial temperatures; c) reaction rate near equilibrium; \tilde{K} kinetic coefficients for various temperatures. One division on the vertical axis corresponds to $2 \times 10^{-13} \text{ sec}^{-1}$.



in which

$$A(t) = - \int_0^t k(\tau) d\tau.$$

Here $k(t)$ and $C^{eq}(t)$ are determined by the cooling law $T(t) = T_0 - St$. For the nonlinear equation (10), the solution can be obtained numerically. Figure 8 illustrates the results for $T_0 = 1473$ K, $S = 10$ K/My. Line 1 is the solution to Eq. (34), while line 2 is the solution to Eq. (38), and line 3 shows the $C^{eq}(t)$ along the $T(t)$ cooling curve.

The following are the frozen values of the mean concentration, the quenching temperatures, and the times to attain C_q for Eqs. (34) and (38) with cooling rate $S = 10$ K/My:

	\bar{C}_q , mol%	T_q , (K)	t_q , My
Diffusion	0.5006	327	114.2
Kinetics	0.5005	974	50.7

Curves 1-3 in Fig. 8 coincide for small t (high T), since the process is almost in equilibrium. The length of that stage, where equilibration occurs, is dependent on the cooling rate and is the longer the slower the cooling. As T falls further, the conversion slows, and the deviation from equilibrium increases up to the time of quenching. Kinetic curve 2 deviates somewhat from

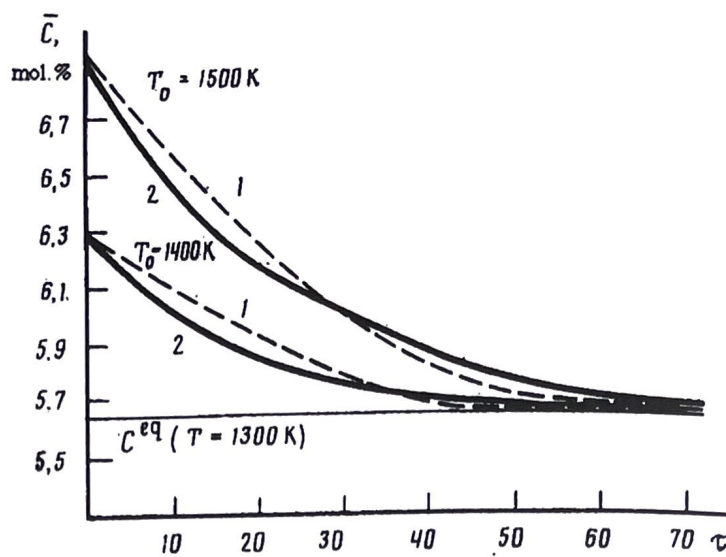


Fig. 6. Mean concentrations of exchangeable component in two models: 1) kinetic equation; 2) diffusion model for isothermal conditions $T = 1300$ K, $T_0 = 1500$ K and 1400 K.

diffusion curve 1 as the deviation from equilibrium accumulates, but the quenched concentrations are almost identical.

The following are results for various cooling modes:

	$S, \text{K/My}$				
$C_q^{dif}, \text{mol}\%$	1749	4126	4558	5006	5481
$C_q^{kin}, \text{mol}\%$	1502	4007	4518	5005	5515
$T_q^{dif}, (\text{K})$	392	392	345	327	298
$T_q^{kin}, (\text{K})$	860	872	922	974	993
$T_c^{eq}, (\text{K})$	459	1067	1128	1195	1270

These show that the kinetic equation is suitable for recovering cooling rates, since the maximum difference between the frozen mean concentrations for the two solutions is ~ 0.04 mol.%. The frozen values can be used as cooling rate indicators.

Figure 9 shows the frozen \bar{C}_q for Eq. (34) (curve 1) and for the kinetic treatment with various S . Figure 10 shows cooling curves and $\bar{C}(t)$ ones for contrasty cooling conditions with $S = 100, 10, 1,$ and 10^{-3} K/My, together with the $C^{eq}(t)$ corresponding to the $T(t)$. The quenching-temperature estimates in this model are completely determined by the reliability of the measurements on the temperature dependence of the diffusion rates and the equilibrium parameters. Therefore, we can reasonably estimate the temperature ranges within which the reaction occurs in a nonequilibrium fashion, i.e., the extent of reaction is governed by the relation between the kinetics and the temperature conditions. The upper bound is the closure temperature T_c and the lower one the quenching temperature T_q .

CONCLUSIONS

1. A new approach is proposed to exchange kinetics, which can be described by equations of Onsager type on the assumption of linearity in the generalized thermodynamic driving forces $\partial G/\partial \zeta$ and fluxes $\partial \zeta/\partial t$.

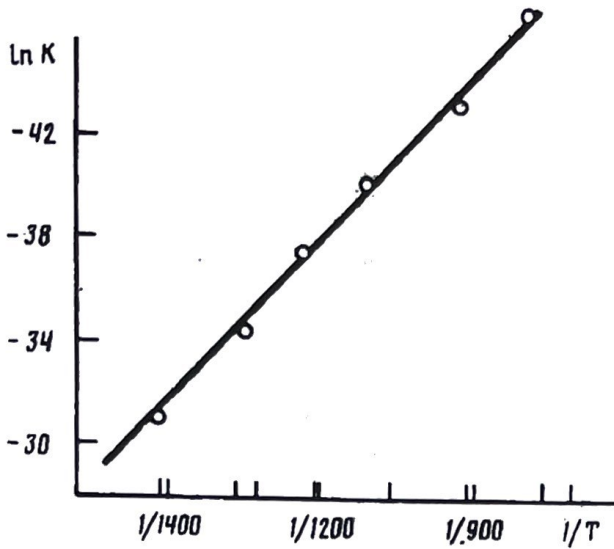


Fig. 7

Fig. 7. Dependence of kinetic coefficient K on temperature. Solid line, linear approximation $\ln K = \ln K_0 - \Delta H_c/RT$.

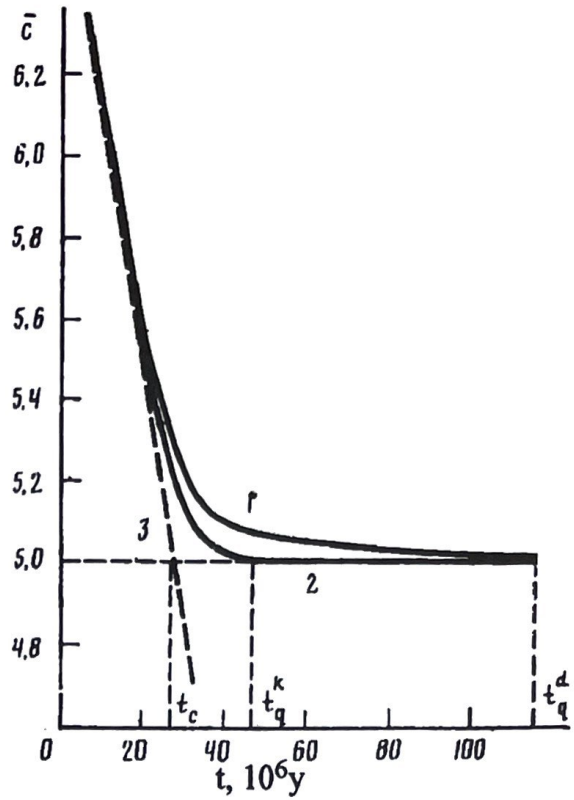


Fig. 8

Fig. 8. Comparison of two models for nonisothermal conditions ($T = T_0 - St$, $T_0 = 1473$ K, $S = 10$ K/My): 1) solution for diffusion; 2) solution to kinetic equation; 3) equilibrium curve. Quenching time t_q , closure time t_c .

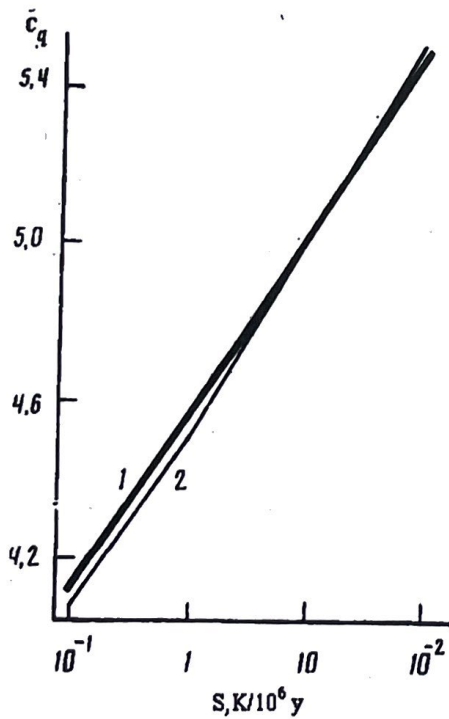


Fig. 9

Fig. 9. Frozen values of mean concentration in relation to cooling rate: 1) diffusion model; 2) kinetic model ($T_0 = 1473$ K).

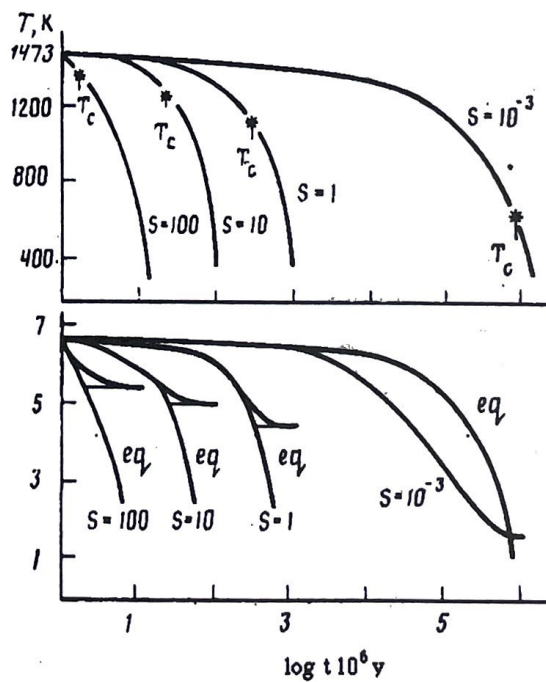


Fig. 10.

Fig. 10. Cooling curves, mean-concentration evolution, and equilibrium curves for various cooling rates.

2. Solid-state ion exchange by bulk diffusion has been used in constructing a first-order kinetic equation relating the reaction rate to the deviation from equilibrium.

3. The kinetic coefficient as a function of model parameters has been examined in dimensionless form: the mutual diffusion coefficients for the components in the phases, the equilibrium constant, and the grain sizes. The parameters have been derived in an Arrhenius equation for the temperature dependence of the kinetic coefficient.

4. Cation exchange with varying temperature has been simulated on the basis of diffusion concentrations averaged over grains instead of diffusion profiles.

5. This model has advantages over earlier ones, as it reduces the uncertainty in determining cooling rates associated with the lack of reliable evidence on diffusion rates at low temperatures; it also enables one to estimate the temperature range in which the reaction occurs in a nonequilibrium fashion and thus to determine the bounds of that range in relation to the cooling rate; in the absence of data on the zoning profiles within the grains, one can use mean concentrations; and in solving complicated geochemical cases, one can avoid complicated calculations associated with solving diffusion equations.

6. The model is applicable to any pair of minerals and enables one to formulate how to measure exchange reactions, particularly in cases where there are considerable difficulties in determining diffusion parameters.

7. The equations have been used to recover cooling rates in metamorphic rocks and to correct and interpret the readings of ion-exchange geothermometers. Criteria have been found for a geothermometer showing either the initial temperature or the closure temperature in a transformation.

REFERENCES

1. Senderov, E. E., L. M. Truskinovskiy, and Ye. A. Mitina, 1991. *Geokhimiya*, No. 1, 121.
2. Senderov, E. E., L. M. Truskinovskiy, and Ye. A. Mitina, 1991. *Geokhimiya*, No. 2, 296.
3. Hopper, R. W., and D. R. Uhlmann, 1976. *J. Geophys. Res.*, **8**, 5721.
4. Onorato, P. J., R. W. Hopper, D. R. Uhlmann, et al., 1981. *Ibid.*, **86**, 9511.
5. Lasaga, A. C., S. M. Richardson, and H. D. Holland, 1977. *Energetics of Geological Processes*, Springer-Verlag, New York, p. 353.
6. Lasaga, A. C., 1979. *Geochim. et Cosmochim. Acta*, **43**, 455.
7. Lasaga, A. C., 1983. *Kinetics and Equilibrium in Physical Geochemistry*, Springer-Verlag, New York, 3, p. 81.
8. Gerasimov, V. Yu., 1988. *Diffuzionnaya zonal'nost' v granatakh kak indikator skorosti temperaturnoy evolyutsii pri metamorfizme [Diffusion Zonation in Garnets as an Indicator of the Temperature Evolution Rate during Metamorphism: Ph. D. Thesis]*, MGU, Moscow. 24 pp.
9. Freer, R., 1981. *Contribs. Mineral. and Petrol.*, **76**, 440.
10. Dodson, M., 1973. *Contribs. Mineral. and Petrol.*, **40**, 259.
11. Truskinovskiy, L. M., A. B. Panferov, and O. L. Kuskov, 1990. *Geokhimiya*, No. 9, 45.
12. Saxena, S., 1975. *Thermodynamics of Rock-Forming Mineral Solid Solutions [Russian translation]*, Mir, Moscow. 205 pp.
13. Crank, J., 1975. *The Mathematics of Diffusion*, Oxford, London. 347 pp.
14. 1981. *Kinetics of Geochemical Processes. Reviews in Mineralogy*, **8**, Mineral. Soc. Amer.
15. S. Groot and P. Mazur, 1964. *Nonequilibrium Thermodynamics [Russian translation]*, Mir, Moscow.